The Anaplastic Lymphoma Kinase Controls Cell Shape and Growth of Anaplastic Large Cell Lymphoma through Cdc42 Activation

Chiara Ambrogio,[1,2] Claudia Voena,[1,2] Andrea D. Manazza,[1] Cinzia Martinengo,[1] Carlotta Costa,[3] Tomas Kirchhausen,[4] Emilio Hirsch,[3] Giorgio Inghirami,[1,2,5] and Roberto Chiarle[1,2]

[1]Center for Experimental Research and Medical Studies, [2]Department of Biomedical Sciences and Human Oncology, and [3]Department of Genetics, Biology, and Biochemistry and Molecular Biotechnology Center, University of Torino, Turin, Italy; [4]Department of Cell Biology, Harvard Medical School, Boston, Massachusetts; and [5]Department of Pathology and New York Cancer Center, New York University School of Medicine, New York, New York

Abstract

Anaplastic large cell lymphoma (ALCL) is a non-Hodgkin's lymphoma that originates from T cells and frequently expresses oncogenic fusion proteins derived from chromosomal translocations or inversions of the anaplastic lymphoma kinase (*ALK*) gene. The proliferation and survival of ALCL cells are determined by the ALK activity. Here we show that the kinase activity of the nucleophosmin (NPM)-ALK fusion regulated the shape of ALCL cells and F-actin filament assembly in a pattern similar to T-cell receptor–stimulated cells. NPM-ALK formed a complex with the guanine exchange factor VAV1, enhancing its activation through phosphorylation. VAV1 increased Cdc42 activity, and in turn, Cdc42 regulated the shape and migration of ALCL cells. *In vitro* knockdown of VAV1 or Cdc42 by short hairpin RNA, as well as pharmacologic inhibition of Cdc42 activity by secramine, resulted in a cell cycle arrest and apoptosis of ALCL cells. Importantly, the concomitant inhibition of Cdc42 and NPM-ALK kinase acted synergistically to induce apoptosis of ALCL cells. Finally, Cdc42 was necessary for the growth as well as for the maintenance of already established lymphomas *in vivo*. Thus, our data open perspectives for new therapeutic strategies by revealing a mechanism of regulation of ALCL cell growth through Cdc42. [Cancer Res 2008;68(21):8899–907]

Introduction

Anaplastic large cell lymphoma (ALCL) is a non-Hodgkin's lymphoma classified among T-cell lymphomas due to the presence of T-cell receptor (TCR) rearrangements at the molecular level and named after the peculiar morphology of its cells (1). The majority of them are characterized by chromosomal aberrations involving the anaplastic lymphoma kinase (*ALK*) gene (2). Most frequently, ALCL carry the t(2;5)(p23;q35) translocation, which fuses the *ALK* gene to the nucleophosmin (*NPM*) gene, resulting in the expression of the oncogenic fusion protein NPM-ALK with constitutive tyrosine kinase activity (3, 4). The NPM-ALK fusion protein plays a key role in the pathogenesis of ALCL, being essential for the survival and growth of lymphoma cells both *in vitro* and *in vivo* (5, 6).

Overall, ALCL cells display cellular shape and phenotype resembling those of activated T cells (7) despite the lack of expression of αβ-TCR heterodimer, CD3ε, and ζ-associated protein 70 (ZAP70), molecules essential to initiate the activation signaling cascade in T cells (8). In ALCL cells, NPM-ALK induces transformation through the activation of pathways shared by the TCR signaling and oncogenic tyrosine kinases, mainly the Ras-extracellular signal-regulated kinase (ERK) pathway, the Janus kinase 3-signal transducer and activator of transcription 3 pathway, and the phosphatidylinositol 3-kinase-Akt pathway (4).

Recent studies have further elucidated the mechanisms by which NPM-ALK can substitute the TCR signaling to control the activation state of lymphoma cells, as well as cell morphology, migration, and cytoskeleton rearrangements (4). We and others have previously shown that NPM-ALK activates proteins involved in the regulation of the cytoskeleton and in cell migration, such as p130Cas (9), SHP2 (10), and pp60Src (11). Recently, the GTPase Rac1 has been shown to regulate the migration of NIH3T3 cells expressing NPM-ALK (12). The Rho-family GTPases are molecular switches that modulate a broad range of cellular processes in T lymphocytes, including activation, migration, proliferation, and generation of the immunologic synapse (13). The regulation of the cytoskeleton is fundamental in lymphoid cells for almost any aspect of T-cell biology, and the Rho-family GTPases are among the major players in this regulation (14). Besides their role in physiologic conditions in lymphocytes, the Rho-family GTPases are thought to contribute to oncogenic transformation and cancer invasiveness of solid tumors (15–17). However, only few reports have thus far implicated the Rho-family GTPases in the development of hematopoietic malignancies. Translocations or point mutations of RhoH have been described in lymphomas and multiple myelomas (18, 19), and loss of Rho function causes thymic lymphomas in mice (20).

In the present study, we show that the activated phenotype of ALCL cells depends on the kinase activity of NPM-ALK, which in turn induces the phosphorylation of the guanine-nucleotide exchange factor (GEF) VAV1 and regulates the activity of the Rho-family GTPases. The NPM-ALK–dependent Cdc42 activation controls lymphoma cell migration, proliferation, and survival *in vitro*. Cdc42 knockdown in ALCL cells affects the establishment and the maintenance of lymphomas *in vivo*. Our data reveal Cdc42 as a novel regulator of lymphoma cell survival, migration, and morphology both *in vitro* and *in vivo*, thus opening perspectives for new therapeutic strategies.

Materials and Methods

Reagents, cell lines, and culture. Human lymphoid cells TS and SU-DHL1 (NPM-ALK positive) and Jurkat and MAC-1 (ref. 21; NPM-ALK negative) were maintained in RPMI 1640 containing 10% FCS. Human

Note: Supplementary data for this article are available at Cancer Research Online (http://cancerres.aacrjournals.org/).

Requests for reprints: Roberto Chiarle, Department of Biomedical Sciences and Human Oncology, University of Torino, Via Santena 7, 10126 Turin, Italy. Phone: 39-11-633-6860; Fax: 39-11-633-6887; E-mail: roberto.chiarle@unito.it.

doi:10.1158/0008-5472.CAN-08-2568

embryonal kidney cells 293T, 293GP, and 293 T-Rex Tet-On (Invitrogen) were maintained in DMEM supplemented with 10% FCS. In 293 T-Rex Tet-On systems, the working concentration of tetracycline in the medium was 1 μg/mL. The specific ALK inhibitor CEP-14083 was kindly provided by Cephalon (22). Secramine A was synthesized in collaboration with G.B. Hammond (University of Louisville, Louisville, KY). For secramine A experiments, cells were grown in RPMI 1640 containing 0.5% bovine serum albumin, 20 mmol/L HEPES, and 0.2% DMSO. Frozen tissues of primary ALK-positive and ALK-negative ALCL were retrieved from the tissue bank of the Surgical Pathology Unit of the University of Torino.

Inducible short hairpin RNA (shRNA) cells were obtained by transduction of pLV-tTRKRAB vector followed by pLVTHM vectors (kindly provided by Dr. D. Trono, Global Health Institute, Ecole Polytechnique Fédérale de Lausanne, Lausanne, Switzerland) containing the shRNA cassettes, as described (23).

Cell lysis, immunoprecipitation, and immunoblotting antibodies. Total cellular proteins were extracted, and cell lysates were used for Western blotting or immunoprecipitation as previously described (9). The following antibodies were used in the study: anti-ALK (Zymed), anti–phospho-ALK (Y1604, Cell Signaling), anti–phospho-Tyr (PY20, Transduction Lab), anti-Rac1 (clone 23A8, Upstate), anti-Cdc42 (C70820, Transduction Lab), anti-RhoA (Santa Cruz Biotechnology), anti–α-tubulin (B-5-1-1, Sigma-Aldrich), anti-VAV1 (R775, Cell Signaling), anti–phospho-VAV (Tyr174, Santa Cruz Biotechnology), anti–phospho-PAK (T423, Biosource), and anti-VAV3 (Cell Signaling). Secondary antibodies were purchased from Amersham.

Immunofluorescence staining. Cells were grown for 12 h on glass coverslips and stained as described (9). Phycoerythrin-conjugated phalloidin (Sigma) was used to stain actin filaments. Nuclei were stained for 10 min at room temperature with bisbenzimide (Sigma). Coverslips were viewed using a Leica TCS SP2 laser-scanning confocal microscope driven by the Leica Confocal Software.

DNA constructs. Wild-type NPM-ALK was cloned in the plasmid vector pcDNA5TO (Invitrogen) at *Hin*dIII/*Xho*I sites and stably transfected into 293 T-Rex Tet-On cells using Effectene reagents as described by the manufacturer (Qiagen). Pallino retroviral vectors containing NPM-ALK or NPM-ALK^{K210R} were previously described (9).

ALK-specific shRNA has previously been described (5). Human Cdc42-specific shRNA sequences (purchased from Open Biosystems, clone ID TRCN0000047628-32) were cloned into the blunt-*Eco*RI site of pLVTHM tetracycline-inducible vector containing the H1 promoter as previously described (5). Clone ID TRCN0000047630 and clone ID TRCN0000047632 were the most efficient in silencing Cdc42 and are indicated as sh-Cdc42 #1 and sh-Cdc42 #2. Human VAV1 specific shRNA sequences were purchased from Open Biosystems (clone ID TRCN0000039858-62). Clone ID TRCN0000039860 and clone ID TRCN0000039858 were the most efficient in silencing VAV1 and are indicated as sh-VAV1 #1 and sh-VAV1 #2.

Retrovirus and lentivirus production, cell infection, cocultures, and chemotaxis. Retroviruses and lentiviruses for cell transduction were obtained as previously described (10). Cells were analyzed for the efficiency of transduction by enhanced green fluorescent protein (EGFP) content on a FACSCalibur flow cytometer (Becton Dickinson). When the efficiency of infection was <80%, cells were sorted on a MoFlo High-Performance Cell Sorter (DAKO Cytomation) to normalize both the intensity of fluorescence and the percentages of transduced cells. For shRNA against VAV1, 24 h after transduction, cells were selected with puromycin for 48 h. Cell cycle analyses and tetramethyl rhodamine methyl ester stainings were done as described (5).

For coculture experiments, ALCL cells and ALCL cells transduced with Cdc42, VAV1, or control shRNAs were mixed in a 1:1 ratio and cultured in standard conditions for 3 wk. EGFP expression was checked over time by fluorescence-activated cell sorting and normalized against the initial time point (day 0). Chemotaxis experiments were done as previously described (9).

Rho GTPase activity assays. Rac1-GTP, Cdc42-GTP, and RhoA-GTP levels were measured by pull-down assays. In brief, cells were washed with cold PBS and lysed in 10 mmol/L $MgCl_2$, 150 mmol/L NaCl, 1% NP40, 2% glycerol, 1 mmol/L EDTA, 25 mmol/L HEPES (pH 7.5), 1 mmol/L phenylmethylsulfonyl fluoride (PMSF), 1 mmol/L Na_3VO_4, and protease inhibitors. Cleared lysates were incubated with 30 μg of glutathione *S*-transferase (GST)-PAK CRIB or GST-mDia fusion proteins (24) conjugated with agarose beads (Upstate Biotechnology) for 30 min at 4°C to detect GTP-loaded Rac1 and Cdc42 or RhoA, respectively. Lysates were then centrifuged, washed, and eluted by boiling in SDS-PAGE buffer for 5 min. Protein levels were detected by Western blotting with the indicated antibodies and quantified by densitometric scanning. The levels of GTP-loaded GTPases were determined by normalizing the amount of GST-bound protein of each experimental point to the amount of GST-bound protein in the control samples.

GEF activity assay. GDP-loaded Rac1 was prepared by incubating 1 μg of affinity-purified GST-tagged Rac1 in loading buffer [25 mmol/L Tris-HCl (pH 7.5), 50 mmol/L NaCl, 0.1 mmol/L DTT, 1 mg/mL bovine serum albumin, and 60 μCi of [8-^{3}H]GDP] at 30°C for 10 min. Thereafter, to inhibit further loading, the sample was added up to 15 mmol/L $MgCl_2$ and placed on ice. For GEF activity measurements, cells (2×10^7) were lysed in 200 μL of a buffer containing 25 mmol/L Tris-HCl (pH 7.5), 1% NP40, 100 mmol/L NaCl, 1% glycerol, 10 mmol/L $MgCl_2$, 1 mmol/L PMSF, 1 mmol/L Na_3VO_4, and protease inhibitors (Roche). Lysates were clarified by centrifugation (12,500 × *g*, 10 min), and 2.4 mg of protein extract were incubated in 300 μL of Rac1GEF buffer [25 mmol/L Tris-HCl (pH 7.5), 1 mmol/L DTT, 1 mg/mL bovine serum albumin, 2 mmol/L GTP, 100 mmol/L NaCl, 1 mmol/L $MgCl_2$] for 5 min at room temperature. To start the reaction, 150 μL of [8-^{3}H]GDP–loaded recombinant Rac1 were added. Samples were analyzed 15 min after incubation at 24°C under shaking. The reaction was stopped by adding 5 mL of ice-cold wash buffer [50 mmol/L Tris-HCl (pH 7.5), 50 mmol/L NaCl, 20 mmol/L $MgCl_2$, 1 mmol/L DTT]. Samples were filtered through a nitrocellulose membrane (0.22-mm pore size, Millipore) under vacuum. The filter was washed twice with 5-mL wash buffer, air-dried, and placed in plastic vials with 5 mL of scintillation mixture (Optima Gold, Perkin-Elmer); bound residual radioactivity was measured using a scintillation counter. Relative GEF activity was represented as the reciprocal function of the residual radioactivity normalized after background subtraction.

Stable isotope labeling with amino acids in cell culture and liquid chromatography-tandem mass spectrometry analysis. For the light cultures, L-lysine:HCl and L-arginine:HCl (Sigma) were added to the amino acid–deficient RPMI; for the heavy cultures, L-arginine:HCl (U-$^{13}C_6$, 98%) and L-lysine:2HCl (U-$^{13}C_6$, 98%9; Cambridge Isotope Laboratories) were added as described (25). TS cells labeled with both L-arginine and L-lysine were treated with 300 nmol/L of a control compound for 3 h, whereas TS cells labeled with both L-arginine-U-$^{13}C_6$ and L-lysine-U-$^{13}C_6$ were treated with 300 nmol/L of the specific ALK inhibitor CEP-14083. Before harvesting, cells were treated for 10 min at 37°C with 100 μmol/L of activated Na_3VO_4. Phosphoproteins were precipitated and samples were analyzed by liquid chromatography (LC)-tandem mass spectrometry (MS/MS) using an easy nanoLC system (Proxeon) interfaced to quadrupole/time-of-flight tandem mass spectrometers (Q-Tof Premier, Waters), as described (25). Protein identification via peptide MS/MS spectra was achieved by using the Mascot software (Matrix Science London) and quantification was done using MSQuant software,[6] as previously described (25).

Microscopy and membrane dynamic assay. Cells were grown in standard conditions, then seeded on glass bottom dishes (WillCo Wells). Cells (2×10^5/mL) were grown in RPMI 1640 without phenol red, supplemented with 20% FCS. After 72 h of culture in a glass-bottomed dish, time lapse was done using a TCS SP2 Leica confocal microscope equipped with a heated chamber for cell culture. Each time lapse was done at least thrice, for at least 8 h running. Dynamic cellular protrusions were manually tracked with MetaMorph (Molecular Devices), and data were plotted with Microsoft Excel. The intersection of the *x* and *y* axes was taken to be the starting point of each cell path.

Mice and *in vivo* experiments. Severe combined immunodeficient (SCID)-Beige mice were purchased from Charles River Laboratories Italia S.p.A. Mice were challenged s.c. in the right flank with 0.2 mL PBS of a single suspension containing 1×10^7 ALCL cells and infected with inducible

[6] http://www.sourceforge.net

Cdc42 shRNA and control shRNA. To induce shRNA expression, mice were fed with 1 mg/mL doxycycline in water for the indicated times. Tumor growth was measured over time. Mice were treated properly and ethically in accordance with European Community guidelines.

Results

NPM-ALK induces an activated phenotype in ALCL cells through F-actin filament remodeling. The activation state of transformed T cells is mirrored by their morphology because signals that originate from the TCR engagement modify cell shape from a round to a polarized shape (13). We first studied the shape and the distribution of actin filaments in cell lines derived from ALCL. The TS cell line displayed a spread morphology and polarized F-actin assembly localized in the lamellipodial membrane protrusions comparable to what observed in TCR-activated Jurkat cells (Fig. 1*A*). Similar results were obtained with SU-DHL1 cells, a second ALCL cell line (data not shown). Notably, the spontaneously activated phenotype in ALCL was dependent on the tyrosine kinase activity of NPM-ALK because TS cells treated with the specific ALK kinase inhibitor CEP-14083 reverted to a round, symmetrical shape and lost the polarization of the F-actin assembly, thus becoming similar to unstimulated Jurkat cells (Fig. 1*A*; Supplementary Fig. S1). Similar changes in morphology after NPM-ALK inhibition were observed in SU-DHL1 and JB6 ALK-positive cell lines (Supplementary Fig. S1) as well as with a different ALK kinase inhibitor (ref. 26; data not shown).

Accordingly to the activated-like morphology and the polarized F-actin assembly, the dynamics of the membrane protrusions was higher in TS as compared with Jurkat cells, which displayed faint and immature membrane protrusions (Supplementary Movies S1 and S2). Again, the dynamics of the membrane protrusions was dependent on the kinase activity of NPM-ALK, given that TS cells

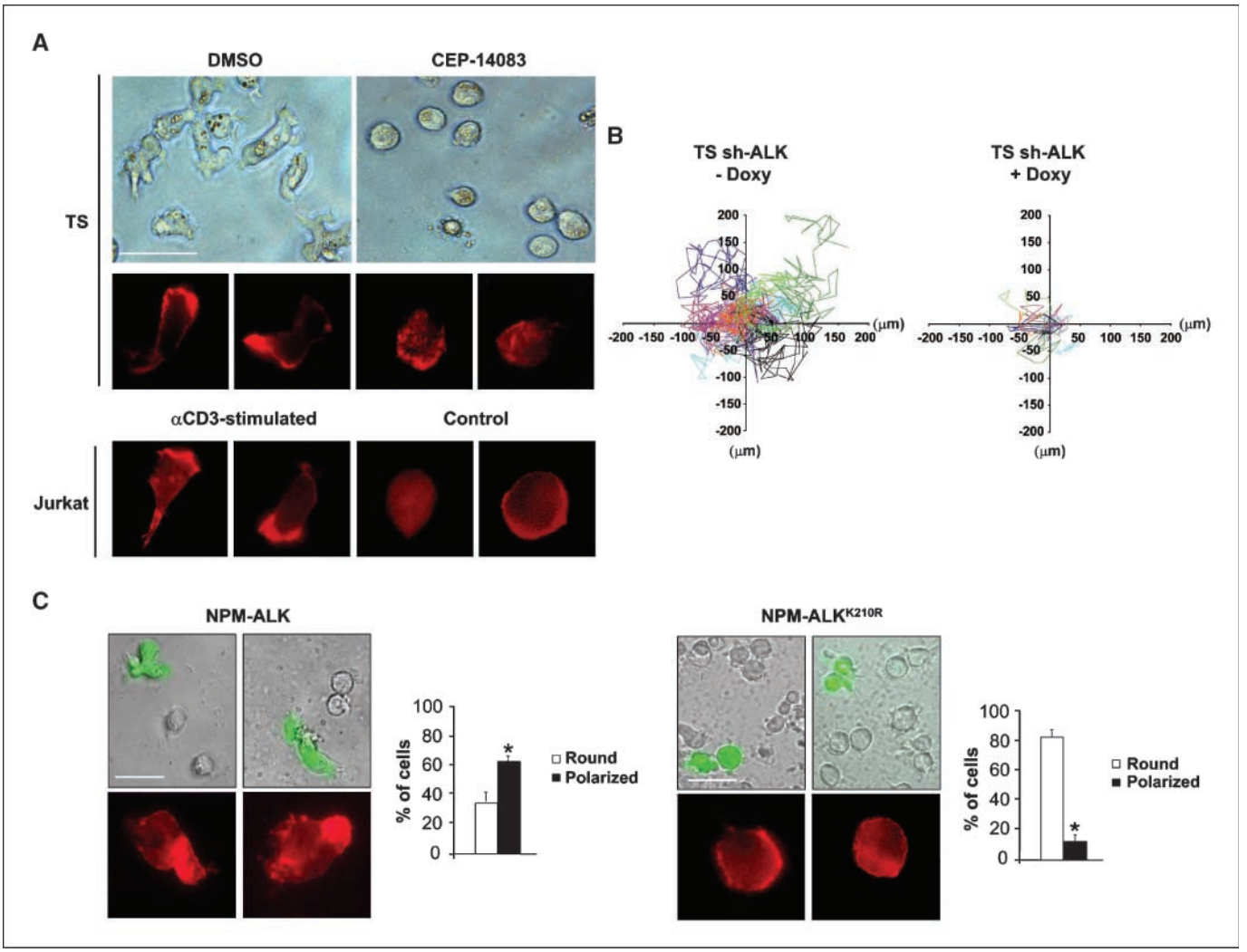

Figure 1. NPM-ALK induces an activated phenotype in ALCL cells. *A,* TS were treated with 300 nmol/L of ALK inhibitor CEP-14083 for 2 h, whereas Jurkat cells were stimulated with immobilized anti-CD3ε antibody (10 μg/mL) for 48 h. Cell morphology was evaluated by contrast-phase imaging (*top*) or by immunofluorescence using phycoerythrin-conjugated phalloidin staining to detect actin filaments (*bottom*). *White bar,* 50 μm. *B,* inducible sh-ALK TS cells were treated with 1 μg/mL doxycycline (*Doxy*) for 84 h. The movements of the membrane protrusions of single cells were traced for at least 8 h at 5-min intervals. Graphs of the movements from 10 representative cells are depicted with different color-coded lines for each different cell. Path lengths in both axes are measured in microns. *C,* MAC-1 cells were transduced with NPM-ALK or NPM-ALK^{K210R} retroviruses carrying EGFP as a reporter. Cell morphology was evaluated by contrast-phase imaging with overlaying fluorescence imaging for EGFP or by immunofluorescence using phycoerythrin-conjugated phalloidin staining to detect actin filaments (*top*). *White bar,* 50 μm. Histograms (*bottom*) represent the percentages of round versus polarized MAC-1 cells transduced with either NPM-ALK or NPM-ALK^{K210R}, quantified by counting at least 100 EGFP-positive cells for each condition. *Columns,* mean; *bars,* SD. *, $P < 0.005$. Data from three independent experiments.

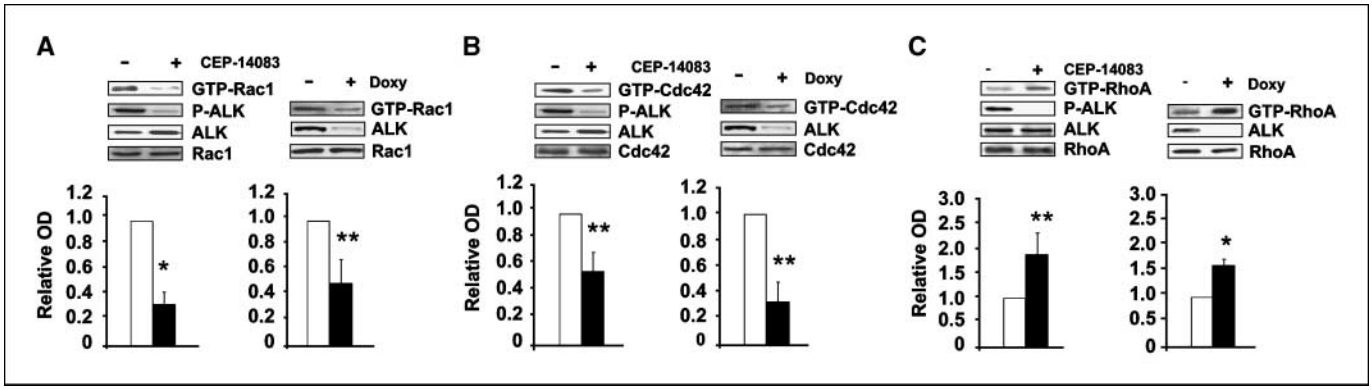

Figure 2. NPM-ALK regulates Rho-family GTPase activation through enhancement of GEF activity. *A* to *C,* wild-type TS cells were treated with 300 nmol/L of ALK inhibitor CEP-14083 for 2 h, whereas inducible sh-ALK TS cells were grown in the presence of doxycycline for 84 h. Total cell lysates were used for Rac1 (*A*), Cdc42 (*B*), or RhoA (*C*) pull-down assays to detect active GTPases. Lysates were also blotted with the indicated antibodies. *Columns,* mean fold changes from 10 independent experiments, quantified by optical densitometry (*OD*); *bars,* SD. *, $P < 0.005$; **, $P < 0.05$ (Student's *t* test).

silenced for NPM-ALK expression (Fig. 1*B*; Supplementary Movies S3 and S4) or treated with the ALK inhibitor (data not shown) showed reduced membrane dynamics. To further prove that NPM-ALK alone is sufficient to determine both changes in morphology and F-actin filaments distribution, we transduced the ALK-negative anaplastic lymphoma cell line MAC-1 with NPM-ALK or the kinase-dead NPM-ALK^{K210R}. After NPM-ALK expression, MAC-1 cells became irregularly shaped with polarized F-actin assembly (Fig. 1*C*), thus confirming the direct role of NPM-ALK in shaping the morphology of transformed T cells.

NPM-ALK activates Cdc42 through VAV1 phosphorylation. To understand the molecular mechanisms by which NPM-ALK induces the activated-like morphology, the polarized F-actin assembly, and the increased dynamics of the membrane protrusions, we analyzed the activity of the Rho-family GTPases in ALCL cells by pull-down assays. When NPM-ALK expression or activity was abrogated by means of specific sh-ALK or the specific kinase inhibitor, the fraction of active Rac1 and Cdc42 significantly decreased, whereas active RhoA increased (Fig. 2*A–C*). Similarly, decreases in the levels of active Rac1 and Cdc42 were observed in

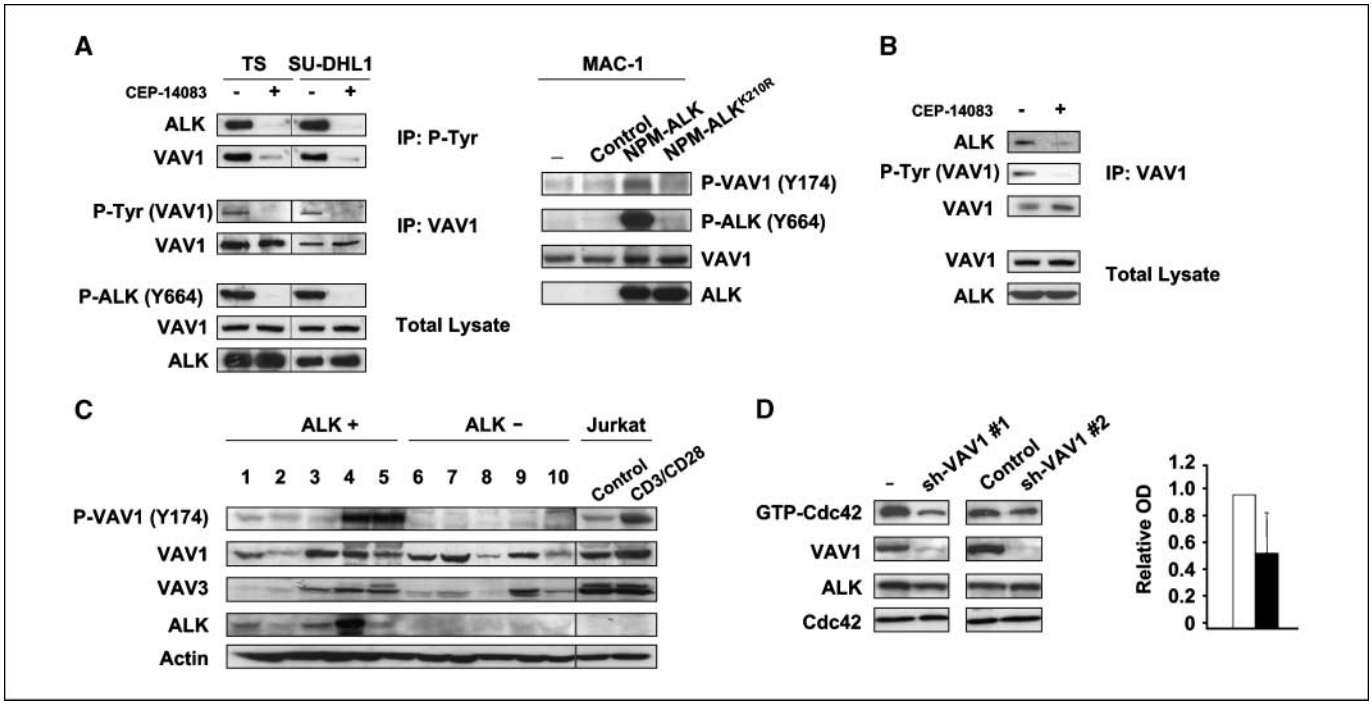

Figure 3. NPM-ALK phosphorylates VAV1 and activates Cdc42 through VAV1 phosphorylation. *A, left,* TS and SU-DHL1 cells were cultured with 300 nmol/L of ALK inhibitor CEP-14083 for 6 h and with orthovanadate for 10 min before harvesting. Total cell lysates were immunoprecipitated with anti-VAV1 or anti–P-Tyr antibodies and blotted with the indicated antibodies. *Right,* MAC-1 cells were transduced with empty vector or with NPM-ALK or NPM-ALK^{K210R} retroviruses. Total cell lysates were blotted with the indicated antibodies. *B,* SU-DHL1 cells were cultured with 300 nmol/L of ALK inhibitor CEP-14083 for 6 h and with orthovanadate for 10 min before harvesting. Total cell lysates were immunoprecipitated with anti-VAV1 antibody and blotted with the indicated antibodies. *C,* frozen tissues from primary ALK-positive (*lanes 1–5*) and negative (*lanes 6–10*) ALCL cases were lysed and blotted with the indicated antibodies. Jurkat T cells were stimulated with CD3 and CD28 for 10 min as a control for VAV1 phosphorylation. *D,* wild-type TS cells were transduced with two different lentiviral constructs encoding for specific shRNAs against VAV1 or a control sequence. Total cell lysates were used for Cdc42 pull-down assay or blotted with the indicated antibodies. Results from one representative experiment. Histograms indicate the quantification by optical densitometry as described above.

SU-DHL1 and JB6 (Supplementary Fig. S2*A*). Consistent changes in Rho-family GTPase activity on NPM-ALK expression were observed also in nonlymphoid cells, such as in HEK293 cells (Supplementary Fig. S2*B*). Thus, in lymphoma, and also in nonlymphoid cells, NPM-ALK seems to control Rho-family GTPase activity in a pattern similar to that described for other tyrosine kinases (27).

To study the mechanisms leading to an increased GTPases activation, we first analyzed the guanine exchange factor (GEF) activity in TS cells where NPM-ALK expression was knocked down by lentiviral inducible sh-ALK. Down-modulation of NPM-ALK resulted in a 40% decrease of GEF activity in ALCL cells (Supplementary Fig. S3). Equivalent results were obtained with TS treated with an ALK inhibitor (data not shown). The most important GEFs in lymphocytes are the VAV family members. VAV1 is selectively expressed in hemopoietic cells whereas VAV2 and VAV3 have a broader pattern of expression (28). The GEF activity of VAV1 is regulated by phosphorylation on tyrosine residues Y142, Y160, and Y174 in the acidic motif (29). This phosphorylation releases an autoinhibitory loop caused by the interaction of the acidic region of VAV1 with the DBL-homology domain, which in turn catalyzes the exchange of GDP for GTP on Rho GTPases (30). By means of stable isotope labeling with amino acids in cell culture and quantitative phosphoproteomic analyses, we identify VAV1 as a protein whose phosphorylated status is strictly dependent on NPM-ALK kinase activity in ALCL cells (Supplementary Fig. S4). In the same analyses, we could not detect phosphorylated peptides of VAV3, which has been suggested to be involved in the NPM-ALK–mediated Rac1 activation (12). By immunoprecipitation and Western blot, VAV1 phosphorylation was strongly reduced in ALCL cells on NPM-ALK kinase inhibition (Fig. 3*A, left*) or NPM-ALK down-modulation in inducible sh-ALK TS and SU-DHL1 cells (Supplementary Fig. S5). Consistently, the forced expression of NPM-ALK, but not of the kinase-dead NPM-ALK^{K210R}, into the ALK-negative MAC-1 cell line resulted in an increase of VAV1 phosphorylation (Fig. 3*A, right*). Because VAV1 has a Src homology 2 domain that can bind to phosphorylated tyrosine residues on tyrosine kinases or adaptor proteins (28), we asked whether NPM-ALK and VAV1 could interact. Indeed, VAV1 coprecipitated with NPM-ALK, and this interaction was strongly diminished when ALCL cells were treated with an ALK kinase inhibitor, indicating a dependence on the kinase activity of NPM-ALK (Fig. 3*B*). We next evaluated the phosphorylation status of

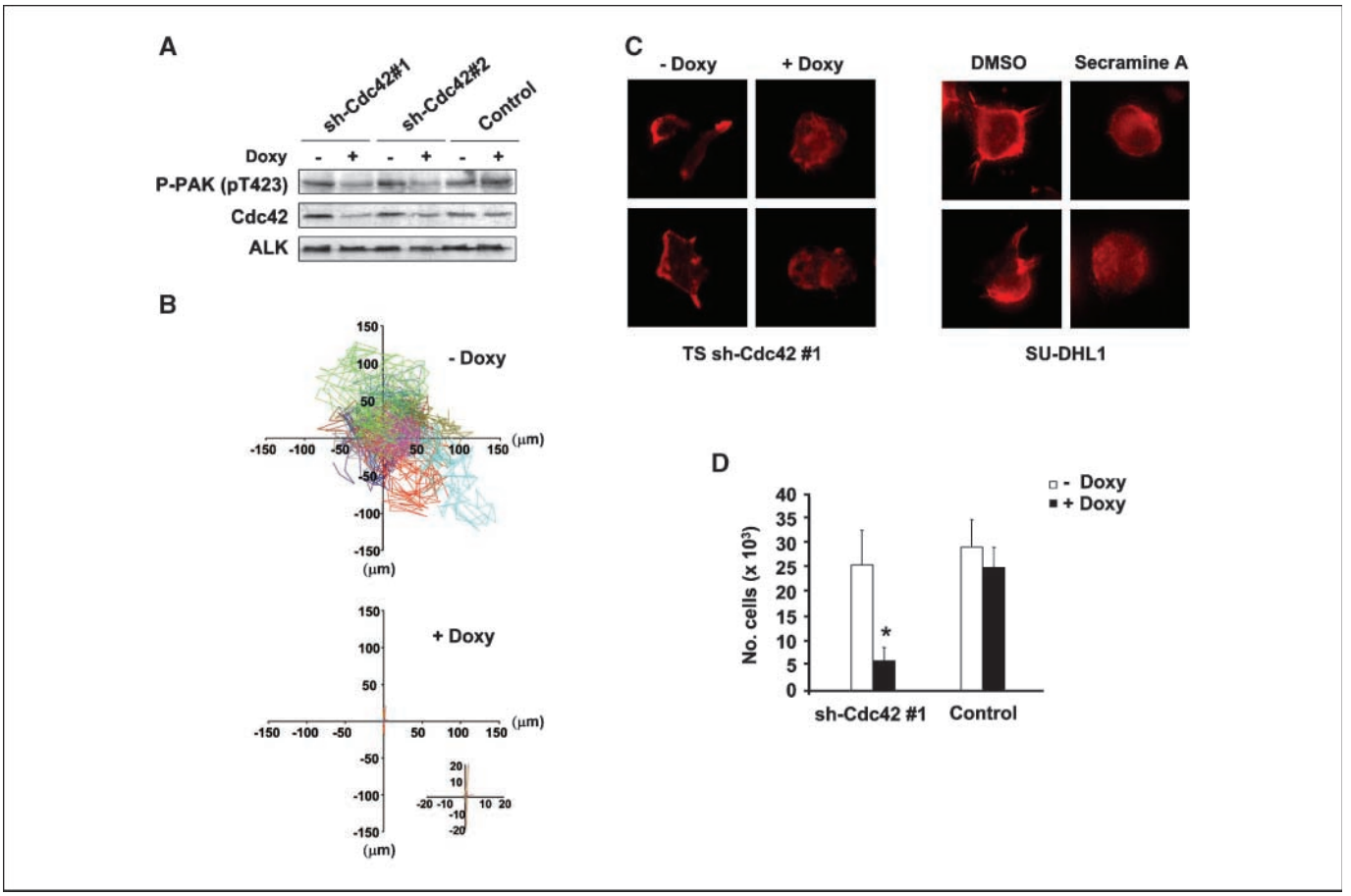

Figure 4. Cdc42 regulates the activated phenotype of ALCL cells. *A,* TS cells were transduced with two different lentiviral constructs inducible for specific shRNAs against Cdc42 and a control sequence. Cells were treated with 1 μg/mL doxycycline for 72 h, then lysed and immunoblotted with the indicated antibodies. *B,* inducible sh-Cdc42 TS cells were treated with 1 μg/mL doxycycline for 72 h. The movements of the membrane protrusions of single cells were traced as indicated in Fig. 1*B*. Path lengths in both axes are measured in microns. *Inset,* a magnified view of the paths of Cdc42-depleted TS cells. *C, left,* inducible sh-Cdc42 TS cells were treated with 1 μg/mL doxycycline for 72 h and then analyzed by immunofluorescence using phycoerythrin-conjugated phalloidin staining to detect actin filaments. *Right,* SU-DHL1 cells were treated with 15 μmol/L of Cdc42 inhibitor secramine A for 1 h and then analyzed by immunofluorescence using phycoerythrin-conjugated phalloidin staining to detect actin filaments. *D,* inducible sh-Cdc42 TS cells were treated with 1 μg/mL doxycycline for 72 h and then used for a transwell assay in response to SDF-1α. *Columns,* mean number of migrated cells; *bars,* SD. Representative graph of three independent experiments done using triplicate wells for each experimental point. Similar results were obtained using the sh-Cdc42 #2 sequence. *, $P < 0.005$ (Student's *t* test).

VAV1 in ALK-positive and ALK-negative primary ALCL. ALK-positive ALCL showed higher amounts of phosphorylated VAV1 as compared with ALK-negative cases, thus strengthening the correlation between NPM-ALK expression and VAV1 phosphorylation (Fig. 3*C*).

VAV1 has an exchange activity for both Rac1 and Cdc42 (31). Therefore, we asked whether VAV1 was responsible for the Cdc42 activation induced by the tyrosine kinase activity of ALK. We knocked down VAV1 expression in ALCL cells by shRNA specific sequences. Two independent sequences that efficiently down-modulated VAV1 expression in lymphoma cells, but not the control sequences, caused a decrease in Cdc42 activity as shown by pull-down assays (Fig. 3*D*), thus indicating that VAV1 is a major GEF involved in the regulation of Cdc42 activity in ALCL cells.

Migration and activated phenotype in ALCL cells depend on Cdc42. Rac1 activity has been recently shown to regulate NPM-ALK–mediated cell migration (12), but the effects of Cdc42 on ALCL cell polarization and activation-associated cytoskeletal rearrangements are unknown. To address this point, we transduced ALCL cells with inducible sh-Cdc42 sequences (Supplementary Fig. S6*A*) and evaluated the activation of the Cdc42 downstream target p21-activated kinase (PAK) with an antibody specific for the autophosphorylated pT423 that is required for PAK activation (32). Indeed, down-modulation of Cdc42 was followed by a decreased phosphorylation of PAK in ALCL cells (Fig. 4*A*). Next, we showed that lymphoma cells knocked down for Cdc42 showed strongly impaired cell dynamics (Fig. 4*B*) and reverted cell morphology to a round, symmetrical shape (Supplementary Fig. S6*B* and Supplementary Movie S5 and S6). Accordingly, Cdc42 knockdown resulted in an impaired polarization of F-actin filaments assembly (Fig. 4*C, left*). Similar effects on the F-actin filaments were observed when cells were treated with secramine A, a recently described selective inhibitor of Cdc42 activity (ref. 33; Fig. 4*C, right*).

Lastly, we asked whether Cdc42 silencing also affects the migration rate of ALCL cells. As expected, Cdc42-knockdown TS cells showed a 5-fold decreased migration rate in response to SDF-1α in a transwell assay as compared with controls (Fig. 4*D*). Altogether, these data indicate that NPM-ALK induces both the activation and relocalization of Cdc42, which in turn regulates the distribution of F-actin filaments and cell migration.

Cdc42 controls ALCL growth *in vitro* and *in vivo*. To further understand the role of Cdc42 in the biology of ALK-positive ALCL cells, we initially evaluated the effects on ALCL cells of a selective Cdc42 inhibitor. Inhibition of Cdc42 activity with secramine A significantly increased apoptosis in ALK-positive as compared with ALK-negative lymphoma cells over time from 6 to 20 h (Fig. 5*A*). These data suggested that Cdc42 could have a major role in the biology of ALK-positive ALCL. Next, we analyzed the growth rate of TS cells knocked down for Cdc42 both *in vitro* and *in vivo*. First, we found that TS cells transduced with the two different inducible sh-Cdc42 sequences had a growth disadvantage compared with TS transduced with the control sequence (Fig. 5*B*). A comparable disadvantage of growth was observed when ALCL cells were knocked down for VAV1 expression (Fig. 5*C*), thus indicating that the integrity of VAV1-Cdc42 pathway is essential for ALCL growth. This growth disadvantage corresponded to an arrest in the G_0-G_1 phases as an early effect on day 4 (Fig. 6*A*), followed by induction of apoptosis (Supplementary Fig. S7). Similar data were obtained with

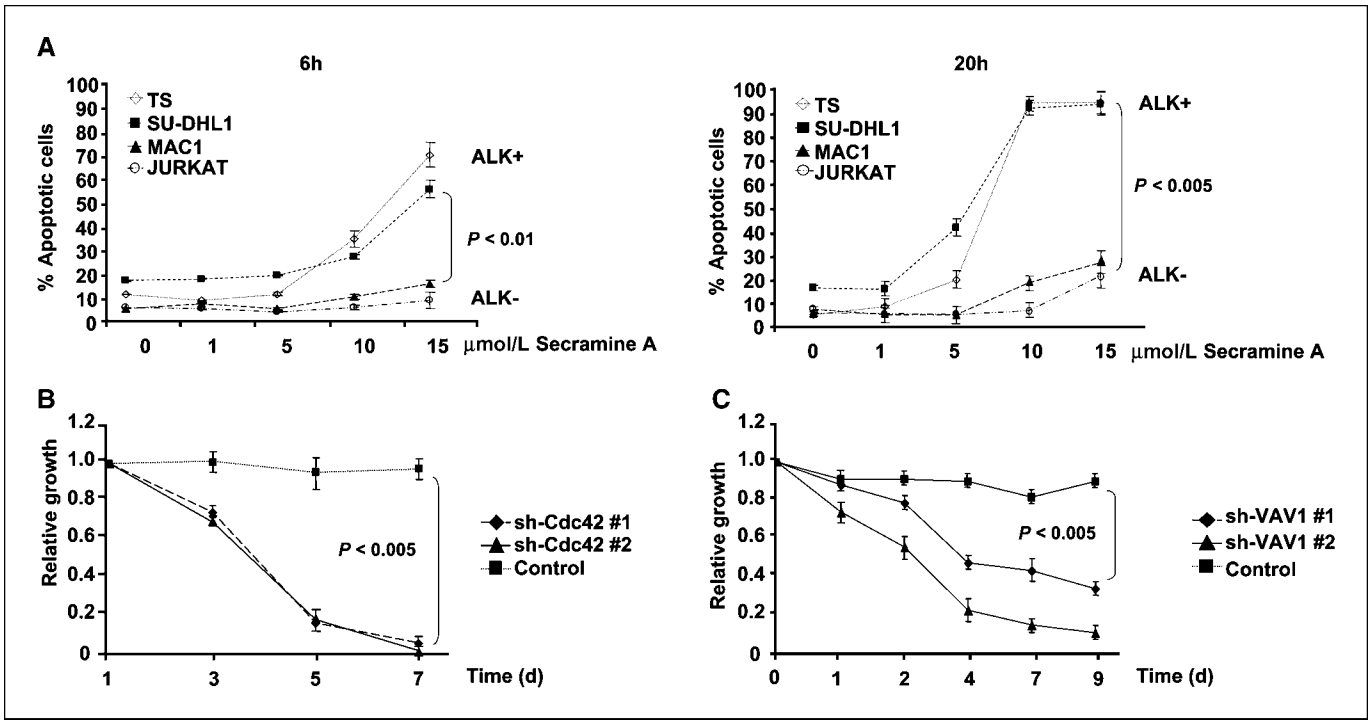

Figure 5. Cdc42 down-modulation impairs the growth rate of ALCL cells *in vitro. A,* ALK-positive (TS and SU-DHL1) and ALK-negative (MAC-1 and Jurkat) cell lines were treated for 6 h (*left*) or 20 h (*right*) with the Cdc42 inhibitor secramine A. Percentages of apoptotic cells were measured by tetramethyl rhodamine methyl ester staining. *B,* inducible sh-Cdc42 TS cells were cultivated in the presence of 1 μg/mL doxycycline for 48 h to induce EGFP expression and Cdc42 down-modulation. Cells were then mixed in a 1:1 ratio with wild-type TS cells and the percentages of EGFP-positive cells were followed over time. *Points,* mean; *bars,* SD. Representative of three independent experiments. *C,* EGFP TS cells were transduced with two different lentiviral constructs encoding for specific shRNAs against VAV1 or a control sequence and selected with puromycin for 48 h. Cells were then mixed in a 1:1 ratio with wild-type TS cells and the percentages of EGFP-positive cells were followed over time. *Points,* mean; *bars,* SD. Representative of three independent experiments.

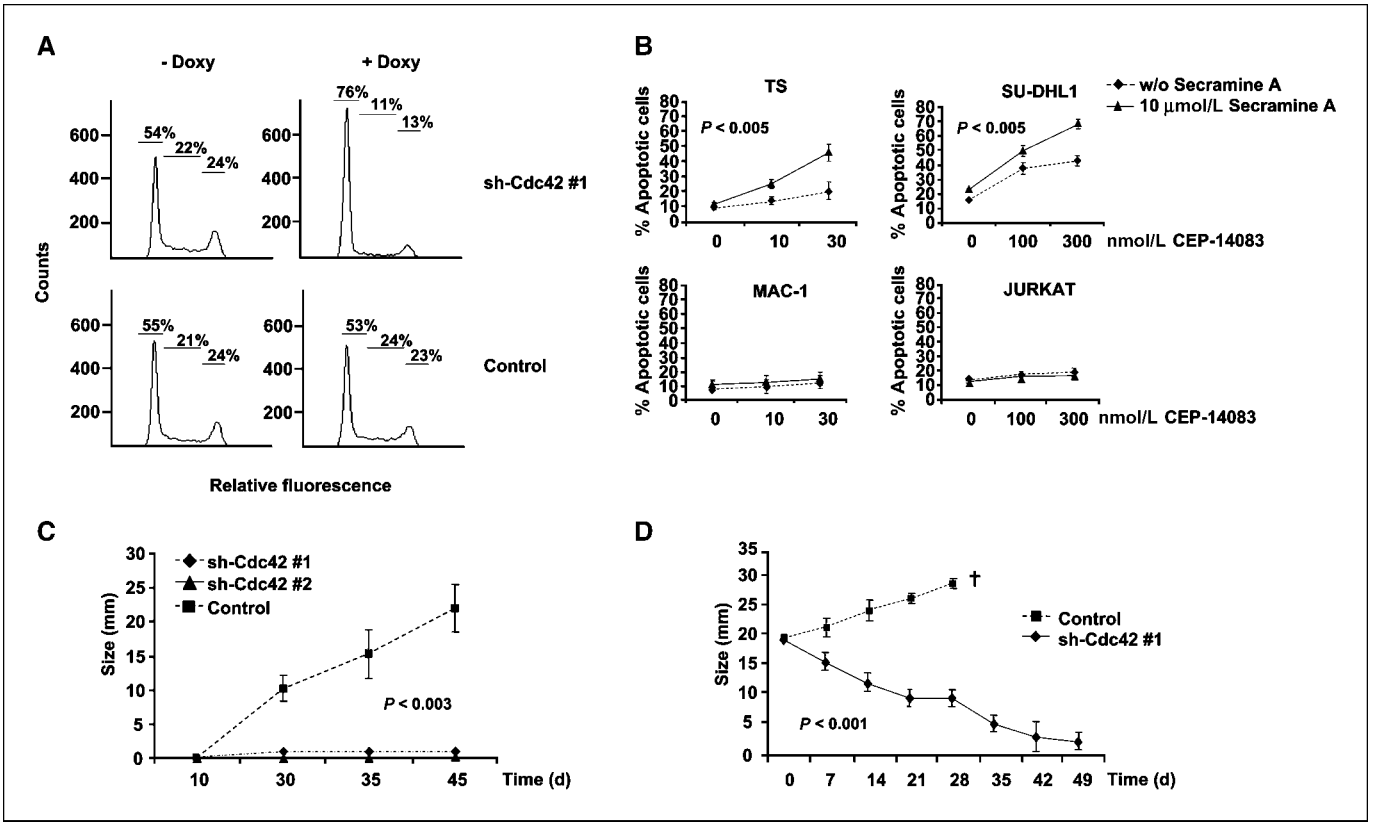

Figure 6. Cdc42 controls the survival and proliferation of ALCL cells *in vitro* and the growth rate of ALCL cells *in vivo. A,* DNA content was analyzed after propidium iodide staining on TS cells transduced with inducible sh-Cdc42 or control sequences after 4 d of induction with 1 μg/mL doxycycline. Data are from one of four independent experiments. *B,* ALK-positive (TS and SU-DHL1) and ALK-negative (MAC-1 and Jurkat) cell lines were treated for 6 h with 10 μmol/L Cdc42 inhibitor secramine A in combination with the indicated concentrations of the selective ALK kinase inhibitor CEP-14083. Percentages of apoptotic cells were measured by tetramethyl rhodamine methyl ester staining. *C,* TS cells (10^7) transduced with either one of the two sh-Cdc42 sequences or with the control sequence were injected s.c. into SCID-Beige immunocompromised mice. Mice were fed with water containing 1 mg/mL doxycycline for the entire time of the experiments. Tumor growth was measured over time. *Points,* mean of at least six mice for each group; *bars,* SD. *D,* TS cells (10^7) transduced with one sh-Cdc42 sequence or with a control sequence were injected s.c. into SCID-Beige immunocompromised mice. When tumors reached a diameter of 20 mm, we started to treat the mice with water containing 1 mg/mL doxycycline. Tumor growth was then measured over time. Mice were sacrificed for ethical reasons when tumors reached the diameter of 30 mm. *Points,* mean from at least three mice for each group; *bars,* SD.

SU-DHL1 lymphoma cells (data not shown). Thus, we showed that Cdc42 is required for lymphoma cell proliferation and survival, findings that highlight a possible role of the Rho-family GTPases in the biology of lymphomas.

Next, we tested whether a combination of ALK and Cdc42 activity inhibitions could result in additive effects on ALCL cells. In fact, ALK kinase activity inhibition through the administration of small molecules is thought to be the new therapeutic weapon that soon will be used to treat ALK-expressing lymphoma patients (4, 34). Indeed, both TS and SU-DHL1 cells showed enhanced sensitivity when treated with a combination of Cdc42 inhibitor with increasing concentrations of an ALK kinase inhibitor, as compared with ALK-negative lymphoid cells (Fig. 6*B*).

Finally, we investigated whether Cdc42 was important also for the growth of ALCL cells *in vivo*. We s.c. injected in immunodeficient mice TS cells inducible for two different sh-Cdc42 sequences or for a control sequence. Doxycycline-treated mice developed rapidly growing tumors only when TS cells were transduced with the control sequence, whereas no growth was observed in mice injected with cells transduced with either the sh-Cdc42 sequences (Fig. 6*C*). These data indicated a role for Cdc42 in tumor establishment. However, more important therapeutic implications could be derived from showing a role of Cdc42 also in tumor maintenance. Therefore, we injected in immunodeficient mice TS cells transduced with inducible sh-Cdc42 as above. When the tumors reached a large size of 2.5 cm, we started to treat the mice with doxycycline. After 7 weeks, tumors derived from sh-Cdc42–transduced TS cells almost completely regressed, whereas control cells kept growing without over effects (Fig. 6*D*).

Discussion

In the present study, we show that ALCL cells display a morphology and activation-associated cytoskeletal rearrangement similar to TCR-stimulated T cells as a consequence of the constitutive tyrosine kinase activity driven by the NPM-ALK fusion. Following activation through TCR ligation, T cells regulate morphology and cytoskeletal rearrangement via a signaling cascade that starts with the phosphorylation of immunoreceptor Tyr-based activation motifs (ITAM) present in each of the TCR-associated CD3 chains. After phosphorylation, the ITAMs recruit ZAP70, and ZAP70 is phosphorylated by Lck. ZAP70, in turn, phosphorylates the adaptor molecules Src homology 2 domain–containing leukocyte protein of 76 kDa (SLP76) and linker for activation of T cells (LAT). Finally, LAT- and SLP76-containing complexes activate the guanine nucleotide exchange factor VAV, which, in

turn, controls the Rho-family GTPases (35). In contrast to normal T cells, ALCL cells are defective for TCR, CD3, and ZAP70 (8) as well as for LAT and SLP76.[7] In the absence of these molecules involved in the TCR signaling propagation, it is supposed that NPM-ALK itself directly regulates the Ras-ERK1/2, phosphatidylinositol 3-kinase-Akt and Src-mediated pathways, thus compensating for the lack of TCR signaling in these cells (4). Here we show that NPM-ALK controls also VAV and Rho-family GTPases activation, thus strengthening the concept that ALK kinase activity compensates for many aspects of TCR signaling.

Rho-family GTPases, mainly Rac1 and Cdc42, play a fundamental role in driving the F-actin remodeling through PAK activation and binding to the Wiskott-Aldrich syndrome protein (WASP) and the WASP-family verprolin-homologous protein-2 (WAVE2), respectively. WASP and WAVE2, in turn, mediate the activation of the actin-related protein 2/3 complex to polymerize F-actin (13). In ALK-positive ALCL, Rac1 has recently been shown to be activated by NPM-ALK and to control the migration of NIH3T3 fibroblasts after forced expression of NPM-ALK (12). Here we show that also Cdc42 serves as a mediator for many relevant biological processes controlled by NPM-ALK in ALCL cells, such as their cell shape and migratory potential, as well as their growth rate.

According to the data here presented, NPM-ALK controls the functions of the GEF VAV1 by phosphorylation to activate Cdc42. Our data obtained by immunoprecipitation suggest that NPM-ALK might form a complex with VAV1 either through a direct binding or through the interaction with adaptor molecules. Among known NPM-ALK adaptor molecules, growth factor receptor binding protein 2 has been shown to bind the NH_2-terminal Src homology 3 domain of VAV1 (28), and p130Cas, which is phosphorylated by NPM-ALK (9), has recently been shown to be involved in VAV1 activation (36). Intriguingly, the findings that the three regulatory tyrosine residues (Y142, Y160, and Y174) of VAV1 are all flanked by an ALK kinase substrate motif (E/D-X-X-Y) raise also the possibility that VAV1 could be a direct substrate of the ALK kinase activity (37).[8] Alternatively, other kinases, such as Src-family kinases, which are activated by NPM-ALK (11), could contribute to VAV1 phosphorylation. The treatment of ALCL cells with the Src-family kinases inhibitor PP2, however, did not change the amounts of active Cdc42 in pull-down assays, thus ruling out a major role for a Src-family kinase member in the Cdc42 activation induced by NPM-ALK (data not shown). Even if we have shown that VAV1 is important in sustaining the activation state of Cdc42 in ALCL cells, our data do not exclude the possibility that other GEFs might also be involved. Colomba and colleagues (12) recently showed that VAV3 mediates the activation of Rac1 in ALCL, without finding evidence for VAV1 activation in their systems. It is possible that these discrepancies could be related either to the different cell lines or to the ALK inhibitor used. In our phosphoproteomic studies, we could not detect changes in VAV3 phosphorylation in contrast to VAV1; instead, we found differentially phosphorylated peptides corresponding to the GEF intersectin 2, both the short and long isoforms (data not shown). The long isoform of intersectin 2 displays specific GEF activity for Cdc42 (38). However, it remains to be determined the role of intersectin 2 in ALCL lymphoma or whether the phosphorylation of intersectin 2 induced by NPM-ALK could enhance its GEF activity. Altogether, these data suggest that NPM-ALK might regulate the Rho-family GTPase activation through different GEFs with different specificities. Downstream of Cdc42, the kinase PAK is a major downstream target (39). Here we show that Cdc42 mediates the activation of PAK in pT423 by phosphorylation in ALCL cells. Accordingly, treatment of ALCL cells with a NPM-ALK–specific inhibitor resulted in a decreased phosphorylation of PAK (data not shown). Thus, PAK activation might represent a mechanism for many of the Cdc42 effects.

Primary ALCL cases expressing ALK show higher amounts of VAV1 phosphorylation than ALK-negative cases (Fig. 3*C*). ALK-positive and ALK-negative ALCL display similar morphology and pattern of growth, but they are now considered as separate entities rather than molecular variants of the same disease.[9] In this view, the mechanisms controlling the morphology, migration, and growth of ALK-negative ALCL are poorly understood and could involve different pathways compared with ALK-positive ALCL.

Along with the control of cell shape and migration, our data strongly support the role of Cdc42 in the establishment and maintenance of ALCL, thus indicating the Rho-family GTPases as new potential therapeutic targets in the treatment of these lymphomas. In fact, our results showed that Cdc42 is essential for the progression of ALCL, mainly regulating lymphoma cell survival and proliferation. Thus, a pharmacologic inhibition of Cdc42 alone or in combination with the inhibition of ALK tyrosine kinase activity could represent the basis for future therapies in ALK-positive ALCL. Currently, Rho GTPases are very promising targets for the development of anticancer drugs (40). Inhibitors of farnesyltransferase, geranylgeranyltransferase I, or hydroxymethylglutaryl (HMG)-CoA-reductase, such as statins, have shown effects on the progression of different solid tumors (40). In keeping with these data, we show that ALK-positive lymphomas could also become an attractive target for specific inhibition of Rho GTPases.

Besides lymphomas, constitutively active ALK following chromosomal translocations has been described also in solid tumors such as inflammatory miofibroblastic tumors and in a fraction of lung carcinomas (41–43). Therefore, it would be interesting to study whether oncogenic ALK induces a similar pattern of GTPases activation in epithelial cells, as well. Moreover, given the similarity in signaling between the oncogenic ALK in tumors and the native ALK receptor in physiologic conditions (2), GTPase activity could be induced by the native ALK receptor in neurons or muscle cells and contribute to neural and muscle cell differentiation (44). Specific studies are needed to address the effects of ALK kinase activity in nonlymphoid cells and to clarify whether Rho-family GTPases could represent a feasible target for therapies also in solid cancers in which ALK kinase is expressed, such as glioblastomas, neuroblastomas, and lung and breast carcinomas (4).

Disclosure of Potential Conflicts of Interest

No potential conflicts of interest were disclosed.

Acknowledgments

Received 7/4/2008; accepted 8/3/2008.

Grant support: NIH R01-CA64033 (G. Inghirami), NIH R01-GM075252-04 (T. Kirchhausen), Ministero dell'Università e Ricerca Scientifica, Associazione Italiana per la Ricerca sul Cancro, European Community (Right Project), Compagnia di San Paolo, Torino (Progetto Oncologia), and Regione Piemonte (Ricerca Sanitaria Finalizzata and

[7] C. Ambrogio, et al., unpublished observations.
[8] http://www.hprd.org/PhosphoMotif_finder
[9] http://socforheme.org/eahp/new.htm

Ricerca Scientifica). C. Voena is supported by a fellowship from the Fondazione Italiana per la Ricerca sul Cancro.

The costs of publication of this article were defrayed in part by the payment of page charges. This article must therefore be hereby marked *advertisement* in accordance with 18 U.S.C. Section 1734 solely to indicate this fact.

We thank Elisa Pellegrino and Matteo Menotti for their invaluable technical assistance, Nicola Crosetto and Carlotta Tanteri for careful reading of the manuscript, Guido Serini and Andrea Bertotti for useful suggestions in confocal images analysis, and G.B. Hammond (University of Louisville) for the help with the secramine A reagent.

References

1. Jaffe ES, Harris NL, Stein H, Vardiman JW. World Health Organization classification of tumors: tumors of the haematopoietic and lymphoid tissues. Lyon (France): IARC; 2001.
2. Pulford K, Morris SW, Turturro F. Anaplastic lymphoma kinase proteins in growth control and cancer. J Cell Physiol 2004;199:330–58.
3. Morris SW, Kirstein MN, Valentine MB, et al. Fusion of a kinase gene, ALK, to a nucleolar protein gene, NPM, in non-Hodgkin's lymphoma. Science 1994;263:1281–4.
4. Chiarle R, Voena C, Ambrogio C, Piva R, Inghirami G. The anaplastic lymphoma kinase in the pathogenesis of cancer. Nat Rev Cancer 2008;8:11–23.
5. Piva R, Chiarle R, Manazza AD, et al. Ablation of oncogenic ALK is a viable therapeutic approach for anaplastic large-cell lymphomas. Blood 2006;107:689–97.
6. Chiarle R, Gong JZ, Guasparri I, et al. NPM-ALK transgenic mice spontaneously develop T-cell lymphomas and plasma cell tumors. Blood 2003;101:1919–27.
7. Rudiger T, Geissinger E, Muller-Hermelink HK. 'Normal counterparts' of nodal peripheral T-cell lymphoma. Hematol Oncol 2006;24:175–80.
8. Bonzheim I, Geissinger E, Roth S, et al. Anaplastic large cell lymphomas lack the expression of T-cell receptor molecules or molecules of proximal T-cell receptor signaling. Blood 2004;104:3358–60.
9. Ambrogio C, Voena C, Manazza AD, et al. p130Cas mediates the transforming properties of the anaplastic lymphoma kinase. Blood 2005;106:3907–16.
10. Voena C, Conte C, Ambrogio C, et al. The tyrosine phosphatase Shp2 interacts with NPM-ALK and regulates anaplastic lymphoma cell growth and migration. Cancer Res 2007;67:4278–86.
11. Cussac D, Greenland C, Roche S, et al. Nucleophosmin-anaplastic lymphoma kinase of anaplastic large-cell lymphoma recruits, activates, and uses pp60c-src to mediate its mitogenicity. Blood 2004;103:1464–71.
12. Colomba A, Courilleau D, Ramel D, et al. Activation of Rac1 and the exchange factor Vav3 are involved in NPM-ALK signaling in anaplastic large cell lymphomas. Oncogene 2008;27:2728–36.
13. Billadeau DD, Nolz JC, Gomez TS. Regulation of T-cell activation by the cytoskeleton. Nat Rev Immunol 2007;7:131–43.
14. Cantrell DA. GTPases and T cell activation. Immunol Rev 2003;192:122–30.
15. Cerione RA. Cdc42: new roads to travel. Trends Cell Biol 2004;14:127–32.
16. Qiu RG, Abo A, McCormick F, Symons M. Cdc42 regulates anchorage-independent growth and is necessary for Ras transformation. Mol Cell Biol 1997;17:3449–58.
17. Wu WJ, Tu S, Cerione RA. Activated Cdc42 sequesters c-Cbl and prevents EGF receptor degradation. Cell 2003;114:715–25.
18. Preudhomme C, Roumier C, Hildebrand MP, et al. Nonrandom 4p13 rearrangements of the RhoH/TTF gene, encoding a GTP-binding protein, in non-Hodgkin's lymphoma and multiple myeloma. Oncogene 2000;19:2023–32.
19. Pasqualucci L, Neumeister P, Goossens T, et al. Hypermutation of multiple proto-oncogenes in B-cell diffuse large-cell lymphomas. Nature 2001;412:341–6.
20. Cleverley SC, Costello PS, Henning SW, Cantrell DA. Loss of Rho function in the thymus is accompanied by the development of thymic lymphoma. Oncogene 2000;19:13–20.
21. Newcom SR, Kadin ME, Ansari AA. Production of transforming growth factor-β activity by Ki-1 positive lymphoma cells and analysis of its role in the regulation of Ki-1 positive lymphoma growth. Am J Pathol 1988;131:569–77.
22. Wan W, Albom MS, Lu L, et al. Anaplastic lymphoma kinase activity is essential for the proliferation and survival of anaplastic large-cell lymphoma cells. Blood 2006;107:1617–23.
23. Piva R, Pellegrino E, Mattioli M, et al. Functional validation of the anaplastic lymphoma kinase signature identifies CEBPB and BCL2A1 as critical target genes. J Clin Invest 2006;116:3171–82.
24. Ray RM, McCormack SA, Covington C, Viar MJ, Zheng Y, Johnson LR. The requirement for polyamines for intestinal epithelial cell migration is mediated through Rac1. J Biol Chem 2003;278:13039–46.
25. Blagoev B, Ong SE, Kratchmarova I, Mann M. Temporal analysis of phosphotyrosine-dependent signaling networks by quantitative proteomics. Nat Biotechnol 2004;22:1139–45.
26. Ahmed G, Bohnstedt A, Breslin JH, et al. Fused bicyclic derivatives of 2,4-diaminopyrimidine as ALK and c-Met inhibitors. Patent. WO/2008/051547.
27. Schiller MR. Coupling receptor tyrosine kinases to Rho GTPases-GEFs what's the link. Cell Signal 2006;18:1834–43.
28. Turner M, Billadeau DD. VAV proteins as signal integrators for multi-subunit immune-recognition receptors. Nat Rev Immunol 2002;2:476–86.
29. Amarasinghe GK, Rosen MK. Acidic region tyrosines provide access points for allosteric activation of the autoinhibited Vav1 Dbl homology domain. Biochemistry 2005;44:15257–68.
30. Aghazadeh B, Lowry WE, Huang XY, Rosen MK. Structural basis for relief of autoinhibition of the Dbl homology domain of proto-oncogene Vav by tyrosine phosphorylation. Cell 2000;102:625–33.
31. Rapley J, Tybulewicz VL, Rittinger K. Crucial structural role for the PH and C1 domains of the Vav1 exchange factor. EMBO Rep 2008;9:655–61.
32. Bokoch GM. Biology of the p21-activated kinases. Annu Rev Biochem 2003;72:743–81.
33. Pelish HE, Peterson JR, Salvarezza SB, et al. Secramine inhibits Cdc42-dependent functions in cells and Cdc42 activation *in vitro*. Nat Chem Biol 2006;2:39–46.
34. Li R, Morris SW. Development of anaplastic lymphoma kinase (ALK) small-molecule inhibitors for cancer therapy. Med Res Rev 2008;28:372–412.
35. Abraham RT, Weiss A. Jurkat T cells and development of the T-cell receptor signalling paradigm. Nat Rev Immunol 2004;4:301–8.
36. Buchsbaum RJ. Rho activation at a glance. J Cell Sci 2007;120:1149–52.
37. Schwartz D, Gygi SP. An iterative statistical approach to the identification of protein phosphorylation motifs from large-scale data sets. Nat Biotechnol 2005;23:1391–8.
38. Wang JB, Wu WJ, Cerione RA. Cdc42 and Ras cooperate to mediate cellular transformation by intersectin-L. J Biol Chem 2005;280:22883–91.
39. Zenke FT, King CC, Bohl BP, Bokoch GM. Identification of a central phosphorylation site in p21-activated kinase regulating autoinhibition and kinase activity. J Biol Chem 1999;274:32565–73.
40. Fritz G, Kaina B. Rho GTPases: promising cellular targets for novel anticancer drugs. Curr Cancer Drug Targets 2006;6:1–14.
41. Soda M, Choi YL, Enomoto M, et al. Identification of the transforming EML4-ALK fusion gene in non-small-cell lung cancer. Nature 2007;448:561–6.
42. McDermott U, Iafrate AJ, Gray NS, et al. Genomic alterations of anaplastic lymphoma kinase may sensitize tumors to anaplastic lymphoma kinase inhibitors. Cancer Res 2008;68:3389–95.
43. Inamura K, Takeuchi K, Togashi Y, et al. EML4-ALK fusion is linked to histological characteristics in a subset of lung cancers. J Thorac Oncol 2008;3:13–7.
44. Mi R, Chen W, Hoke A. Pleiotrophin is a neurotrophic factor for spinal motor neurons. Proc Natl Acad Sci U S A 2007;104:4664–9.